

Electric Field Induce Blue Shift and Intensity Enhancement in 2D Exciplex Organic Light Emitting Diodes; Controlling Electron-Hole Separation.

Hameed A. Al Attar and Andy P. Monkman

Department of Physics, Durham University, Durham, DH1 3LE, United, Kingdom

Abstract

In donor-acceptor type organic optoelectronics devices such as organic solar cell (OPV) and exciplex type organic light emitting diode (EOLED), charge transfer (CT) mechanism is the main process that leads to Coulombically bound charge pair (geminate pair) which either dissociate into free charge carriers or relaxes down to form an emissive exciplex. Extensive theoretical and experimental works build on Onsager calculation to determine the initial electron-hole distance and to study the effect of the electric field on the geminate pair dissociation and free carrier's generation. Here we discuss the reverse Onsager process where the field induces blue spectral shift emission as the e-h distance reduced. Solving the field effect Coulomb potential energy equation, we were able to explain the observed blue spectral shift and determined the e-h distances, Coulomb potential energy and the electric field distribution in the device structure. The process provides fundamental understanding of the exciplex recombination at the donor-acceptor interface.

Organic optoelectronic devices have many current technological and future potential applications, for example in flat-panel displays, large area lighting, photovoltaics, field-effect transistor and sensors ^[1]. An important 'new' class of organic optoelectronic devices are those where charge and energy transfer (CT and ET) between donor and acceptor molecules is involved ^[2]. The general term for such bimolecular CT excited states is an exciplex ^[3]. Examples of such devices are the organic photovoltaic cell (OPV) and exciplex type organic light emitting diodes (EOLED). Recently, interest in EOLEDs has grown because highly efficiency exciplex devices of blended single layer D-A materials with external quantum efficiency up to 11.3% have been reported ^[4-6]. Fluorescent or phosphorescence emitter molecule guests in an exciplex host system also show greatly enhanced emission^[7] with devices demonstrating external quantum efficiencies exceeding 30% being reported ^[8]. Understanding the CT mechanism and exciplex excited states in OLEDs is thus of crucial importance to enable optimisation of device efficiencies. CT is influenced by the HOMO-LUMO energy offset of the D and A molecules as well as the local interface morphology ^[9]. The exciplex energy is strongly dependent on the wave-function overlap of the electron and hole on the A and D that form the CT state. While the EOLED requires stabilised, strong electron-hole wave-function

overlap in the exciplex to yield efficient radiative recombination, an OPV requires weakly bound electron-hole pairs with poor wave-function overlap *i.e.* as in a hot CT state, in order to easily separate to form free charge carriers^[10]. Stabilisation of the electron-hole pair depends on the coulomb attraction between the charges which in turn depends on the electron-hole separation. Intermolecular charge transfer is known to be short range in organic materials. Estimation of the average electron-hole distance and quantification of the degree of charge-transfer character has been the subject of previous experimental and theoretical studies^[11]. Conwell *et al*, carried out Monte Carlo simulations of the chain packing and inter chain excitations in PPV derivatives, resulted in 3.3-4.2 Å interchain charge separation^[12]. Recently attention has turned to exciplex states in the solid-state^[13, 14], Muntwiler and co-workers^[15] have presented an experimental and theoretical model for CT excitons at the surface of crystalline pentacene using time-resolved two-photon photoemission spectroscopy. They identified discrete CT exciton energy states of 1s, 2s and 3s characters which are bound by discrete coulomb energies of 0.43, 0.21 and 0.12 eV, respectively, in agreement with simplified quantum mechanical modelling. Sharifzadeh *et al*^[14] have computed the average electron-hole distance and quantify the degree of charge-transfer character within optical excitations in solid-state pentacene. They show that several low-energy singlet excitations are characterized by a weak overlap between electron and hole and an average electron-hole distance greater than 6 Å.

Separation of such geminate CT states into free charges which is a prerequisite for any solar cell, is enhanced by an external electric field^[16]. The yield of optical charge carrier generation as a function of external electric field (F) can be interpreted in terms of classical Onsager theory of geminate recombination^[17, 18]. The energy of a thermalized photoexcited electron-hole pair, remaining coulombically bound (geminate), that undergo a Brownian random walk within a potential well formed by a superposition of the coulomb potential of the pair, and an external electric field F , is given by;

$$E_C(r) = -\frac{e^2}{4\pi\epsilon_0\epsilon r} - eF \cdot r \quad (1)$$

Where r is the electron-hole separation, e is the elementary charge, ϵ_0 is the dielectric permittivity, and ϵ is the relative dielectric constant. The initially photocreated unrelaxed 'hot' excited states have an initial electron-hole separation distance of r_0 , These either relax down

into the coulomb potential well to form a (relaxed) exciplex state or dissociate to form free carriers. Onsager theory predicts strong dependencies for the electron–hole dissociation probability on both external electric field and temperature ^[17]. Whereas there has been extensive research on exciplex fluorescence quenching by an electric field and extrinsic carrier photogeneration in heterojunctions ^[19], there are no reports of the opposite process occurring; where the applied field acts to increase the electron-hole confinement.

The estimated initial electron–hole separation of geminate pairs obtained from exciplex fluorescent quenching was ~ 2-3 nm for poly (N-vinylcarbazole) film doped with different acceptor molecules. Morteani *et al* ^[20] determined the geminate pair separation to be 2.2 nm for (TFB:F8BT) and ~ 3.1nm for (PFB:F8BT) and that the process was only slightly temperature dependent. Arkhipov *et al* ^[21] suggested a model for temperature-independent photogeneration of charge carriers in conjugated polymers. All the above work focused on the investigation of the relatively long range electron–hole separation that leads to dissociation. Here we use a new approach to explore the evolution of the relaxed exciplex when an external electric field *reduces* the electron–hole separation and *increases* emission, at an abrupt donor-acceptor interface. The technique employs OLED devices with a D-A interface having a relatively high HOMO-LUMO energy offset. The injected electrons and holes cannot overcome this high interface potential barrier leading to the formation of a significant density of exciplex states ($|D^+A^->$), in a 2D sheet, pinned across the interface.

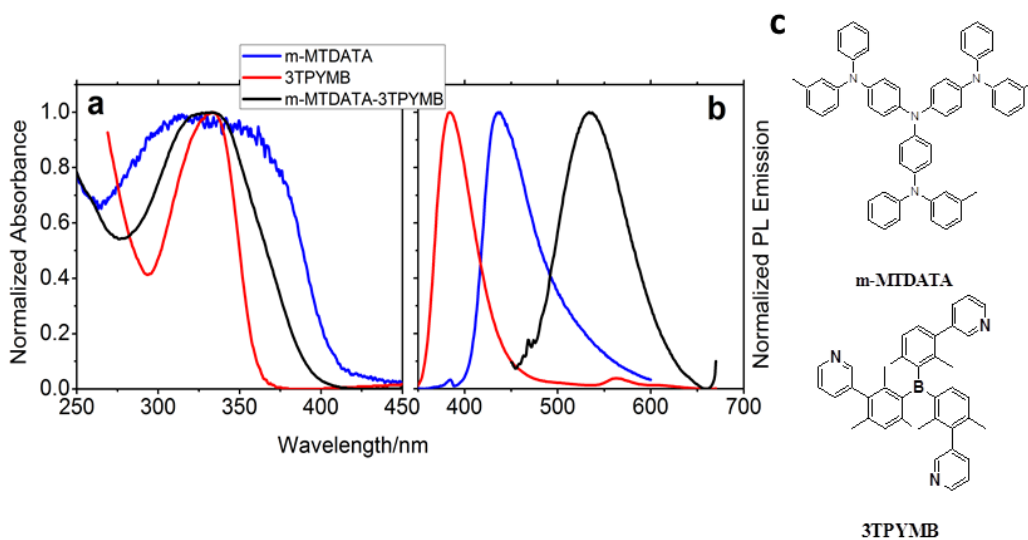


Figure 1. Normalised UV-vis-absorption (a) and PL (b) spectra of m-MTDATA, 3TPYMB and their 1:1 ratio blended spin coated films. The excitation wavelength for the PL spectra was 337 nm. (c) The chemical structure of m-MTDATA and 3TPYMB.

The absorption and emission photoluminescence (PL) spectra of the individual 4,4',4''-tris[3-methyl phenyl(phenyl)amino] triphenylamine (m-MTDATA) donor and tris-[3-(3-pyridyl) mesityl]borane (3TPYMB) acceptor, and of 1:1 weight ratio of blended m-MTDATA: 3TPYMB films are shown in Fig. 1. The absorption spectra of the m-MTDATA: 3TPYMB blend films Fig. 1a, is found to be a linear combination of the individual constituents. This indicates no ground state complex formation or aggregation which would show a new absorption feature or a shift in the absorption spectrum of the blend film. The PL spectra in Fig. 1b, shows a broad featureless emission, peaked at 540 nm for the blend film which is

significantly redshifted compared with the individual emission of the m-MTDATA and 3TPYMB at 442 and 390 nm respectively. Since the blend film does not show a new absorption band, therefore this red shifted broad emission band may be assigned to emission from an exciplex species. Exciplex excited states are formed out off a linear combination of the possible excited states of the D-A system, i.e. charge transfer $|D^+A^->_{CT}$ and locally excited states, $|D^*A>_{Loc}$ and $|DA^*>_{Loc}$ ^[22]

$$\Psi_{Exc} = c_1|D^*A>_{Loc} + c_2|DA^*>_{Loc} + c_3|D^+A^->_{CT} \quad (2)$$

Where c_n represent the contribution of each configurations to the overall excited state.

The LUMO and HOMO energies of m-MTDATA and 3TPYMB, taken from the literature^[4], indicate an interface having a relatively high HOMO-LUMO energy offset, ΔE ($\Delta E_{LUMO} = 1.3$ eV and $\Delta E_{HOMO} = 1.7$ eV). Referring to the absorption spectra of fig. 1a; one can expected that both m-MTDATA and 3TPYMB strongly absorb 337 nm excitation light, and the excited molecules generate near 100% exciplexes because $\Delta E \gg$ excitonic binding energy ~ 0.5 eV. Furthermore, the triplet energy levels for the donor and the acceptor^[4] are both higher than the exciplex states giving pure CT ($|D^+A^->$) emission.

To investigate the m-MTDATA: 3TPYMB exciplex state in more detail, time resolved emission was studied, fig. 2a, and was compared with a system having a far shallower HOMO-LUMO energy level offset (< 0.3 eV) *N,N'*-dicarbazolyl-3, 5-benzene and 2, 2',2''-(1, 3, 5-benzenetriyl)tris(1-phenyl)-1H-benzimidazol (mCP:TPBi) fig. 2b. To exclude any contribution from prompt (D or A) exciton fluorescence we ignored the first ten nanoseconds in the log-log plot of figure 2. Figure 2a clearly shows that the m-MTDATA: 3TPYMB system is entirely dominated by exciplex emission, from 10 ns on, whereas the mCP:TPBi system shows two distinct emitting species with widely separated emission spectra and decay times. A long lived species emitting in the red having near 100% CT character, whereas the shorter lifetime component emits more strongly in the blue, close to the exciton emission wavelength of the

donor, and is postulated to arise from delayed fluorescence arising from triplet fusion, because both mCP (2.9 eV)^[23]and TPBi (2.73 eV) ^[6] have slightly lower triplet energies than the exciplex energy (2.92 eV). A more extended discussion on this competition between TADF and TTA and the effect of HOMO-LUMO energy level offset will be given in a forthcoming paper.

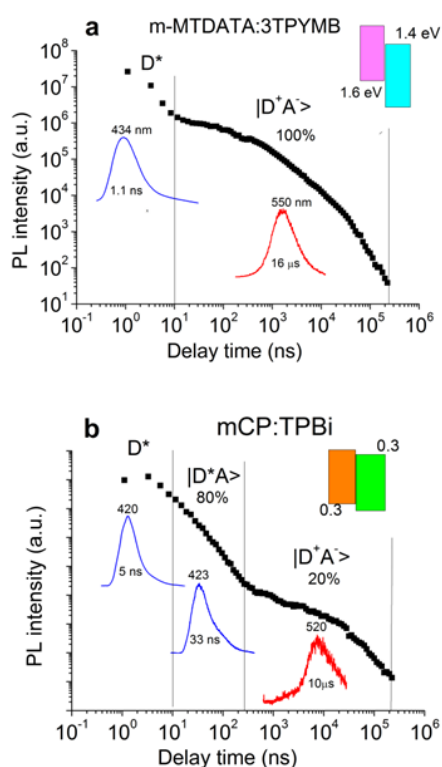


Figure 2. PL decay transient of co-evaporated 1:1 thin film of MTDATA: 3TPYMB (a) and mCP:TPBi (b) using a spectrograph and gated iCCD camera. The percentage contribution calculated as the area under the corresponding partial decay curve. Excitation wavelength was 355 nm from third harmonic of Nd-YAG laser, with emission band shape and position given for the relevant time regions. Insets schematically depict the band offsets at the junctions of each DA pair.

To study the effect of the electric field on the exciplex states pinned across the interface, single and double layer OLED devices were prepared. The double layer, ‘abrupt interface’ device (DL) structure was ITO/PEDOT: PSS (40 nm) / m-MTDATA (30 nm) / 3TPYMB (30 nm) /

LiF(0.8 nm)/Al(100 nm) and the single layer (SL) device structure was ITO/PEDOT:PSS(40 nm)/ MTDATA:3TPYMB 1:1 (co-evaporated 30 nm)/ 3TPYMB(30nm) / LiF/Al.

Figure 3, shows the exciplex emission from the DL devices at different applied voltage. The emission wavelength is strongly blue shifted from 550 nm at 2.3 V bias to 504 nm at 8 V bias. At higher applied voltage >8 V the blue emission shift converges to 500 nm (SI 1), *mainly due to lack of resolution in measuring the spectral shift*. The blue shifted emission could be attributed to donor emission as a result of Auger recombination^[24]. However, this is not the case for two reasons; first, no emission was observed at the donor emission peak of 436 nm, even at the highest applied voltage (fig. 3a.). *This is because, m-MTDATA is a rich hole donor, therefore only exciplex emission is observed^[24]. Secondly, the blue shifted emission is simply following the interface potential energy characteristics, i.e. the shift rate is high when the relative e-h separation is large, and decreases at the interface potential barrier is approached (where the blue emission shift converges to 500 nm (fig. 3b)). The blue emission shift convergence is strong evidence of an interface potential energy effect on electron-hole separation. This blue spectral shift is reversible and unaffected by temperature (in the range 290K – 350K), which indicates no chemical degradation of the donor or acceptor molecules or molecular re-arrangement at the interface.

*To consider the universality of the phenomenon, two further D-A pairs with large HOMO-LUMO energy offset was tested. Smaller blue emission shift were observed as depicted in *fig SI-2, which indicates that the zero field electron-hole separation is not only dependent on the HOMO-LUMO energy offset but also on the relative geometric orientation of the donor and acceptor molecules at the interface. These results agreed with previous studies on the effect of geometric structure at organic-organic interfaces on the efficiency of exciton-dissociation and charge separation processes in D/A type solar cells ^[25].*

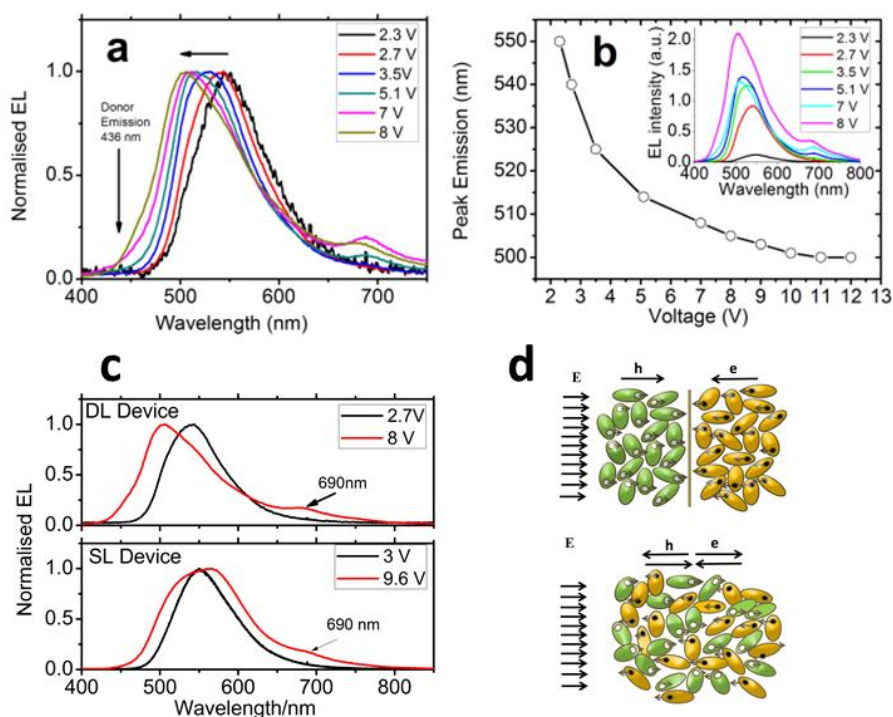


Figure 3. (a) Show the exciplex emission from DL device at different applied voltage. (b) Emission wavelength is blue shifted from 550 nm at 2.3 V to 500 nm at 12V, inset: The real non-normalised plot of the spectral shift showing the strengthening intensity. (c) OLED devices at low and high applied voltage for double layer (DL) and single layer (SL). (d) Illustrate the effect of the electric field on the electron-hole distance and hence spectral emission shift.

Comparing the initial electrically generated exciplex emission peak at 550 nm (2.3 V bias) with that observed with optically excitation in bulk blend film, peak emission at 540 nm (effectively zero bias), one can ascribed the 10 nm red shift of the (2.3 V) electrical generated states to the effect of the built-in potential across the junction due to the electrode work-function off-set which acts to oppose the applied bias. This was confirmed by measuring the emission peak from the device interface states using optically excitation and a multiple interface structure, where the emission was observed at 550 nm (Fig SI-3). We find that a forward biased voltage

of 2.7 V is required to shift the (device) exciplex emission peak back to 540 nm. This yields an estimation of a built-in potential of 0.4 V which is in agreement with the estimated room temperature value based on the band bending effect on the ITO and LiF/Al work function [26]. However, this estimation can only be considered as qualitative and an indication of built-in potential. Along with the blue shift of emission, the emission band gains some structure. This reflects a decrease in the overall electron-hole separation, leading to a decrease in $|D^+A^->_{CT}$ character of the excitation, and concomitant increase in $|D^*A>_{Loc} + |DA^*>_{Loc}$ character of the exciplex. This will have the effect of increasing the radiative decay rate, k_f , of the exciplex^[11].

$$k_f \propto \tilde{\nu}_{av} \left(\frac{\tilde{\nu}_{av}}{\tilde{\nu}_{D^*} - \tilde{\nu}_{av}} \right)^2 \quad (3)$$

where the $\tilde{\nu}$'s represent the average energy of the donor and the exciplex emission respectively.

Generally, the exciplex emission maximum is related to the ionization potential of the donor (I_D), electron affinity of the acceptor (A_A) and stabilized by the electron-hole coulomb potential energy (E_C)^[27]

$$h\nu_{EX}^{max} \approx I_D - A_A - E_C \quad (4)$$

Where the electron-hole coulomb potential energy under an external electric field F can be represented by Equation (1). Equation (1) and (4) predicted that the blue shift of the EL should be entirely due to an increase in the coulomb energy E_C and concomitantly to a reduction in the electron-hole separation upon applying the forward applied voltage which acts in the opposite direction to the dipole moment of the CT state. Thus to observe such a shift the CT states must be uniaxially aligned with the field, i.e. a 2D sheet of exciplex states, pinned across an abrupt interface.

Comparing the DL device behaviour to that of the single 'blend' layer devices, figure 3c, we see that the blue shift of the EL is only observed in the DL devices. In the single emissive layer the device emission at high applied voltage shows a broadening on both sides of the emission

band when compared with the EL profile at low applied voltage figure 3c. This behaviour can be explained as shown in the sketch in figure 3d. Assuming that the injected electrons and holes reside on the acceptor (LUMO) and donor (HOMO) respectively at the interface which they cannot cross because of the large potential offsets at the junction, and the molecules are randomly distributed near the interface. Upon applying the electrical field the force exerted on the exciplexes in the double layer device causes an average decrease in electron-hole separation and concomitantly the EL spectrum blue shifts to shorter wavelength (higher energy) according to equations 1 and 4. In contrast the force exerted by the field on the randomly oriented exciplex dipole moments in the single layer device leads to both increasing and decreasing electron-hole separation. This causes an overall increase in the energy dispersion of the exciplex states and a broadening of the EL emission, as indicated in figure 3 (SL Device). Further, at higher drive bias, a new peak at 690 nm appears, which is *irreversible*, which has been termed an electomer or electroplex in past literature [28]. The device efficiency and brightness of the SL device is much higher than that for the DL device due to far larger effective interface area in the blended system compared to a single heterojunction interface *Fig SI- 4.

Normally, an applied electric field causes extrinsic carrier generation and PL quenching [19-21, 29]. Such measurements emphasize electron-hole dissociation which is dominated by the second term in equation 1. At the abrupt interface with directionally pinned exciplex states across the junction the forward bias voltage is not great enough to drive the electrons and holes across the interface because of the high potential barriers due to the very large HOMO-LUMO energy off-sets, so the electron-hole separation becomes smaller, but the exciplex states are not quenched, and the coulomb potential energy is explicitly dominated by the first term of equation 1. To model the observed EL blue shift and determine the change in electron-hole separation as a function of applied voltage, equation 1 should be solved at the relaxed CT

exciplex energy (equilibrium electron-hole separation) where the change in the Coulombic potential energy is constant. Writing equation 1 in units of eV, we get

$$E_C = \frac{A}{r} + rF \quad (5)$$

$$\text{Where } A = \frac{e^2}{4\pi\epsilon_0\epsilon}$$

At the relaxed CT exciplex point

$$\frac{dE_C}{dr} = 0 \quad \therefore F = A/r^2 \quad (6)$$

$$\text{And,} \quad r = 2A/E_C \quad (7)$$

Knowing E_C from the exciplex peak emission wavelength using relation 4, taking $I_D = 5.1$ eV, $A_A = 3.3$ eV^[4] and the average relative dielectric constant ϵ for the D-A is assumed to be 3.5.

The experimental data and the calculated parameters from relations 5-7 for different applied voltage are shown in table-1.

Knowing the electric field, F , a plot of equation (5) for different applied voltage can be given, figure 4a. Table 1 and figure 4a clearly show how the exciplex characteristics and the observed blue shift change as a function of applied voltage in the vicinity of the interface. Figure 4b, shows the HOMO-LUMO energy level diagram across the interface and the scale of the variation of electron-hole separation with applied field with respect to the interface. This approach allows us to measure very sensitively the evolution of the electron-hole distance with field from the exciplex emission wavelength. The effective thickness over which the field acts was calculated from V/F , where an average distance of ~ 33 nm is obtained, table 1. Since the double layer device (DL) structure is ITO/PEDOT: PSS (40 nm) / m-MTDATA (30 nm) / 3TPYMB (30 nm) / LiF(0.8 nm)/Al(100 nm), we can assume that the electric field is distributed homogeneously across the donor-acceptor layers which give an effective average at the middle of each layer.

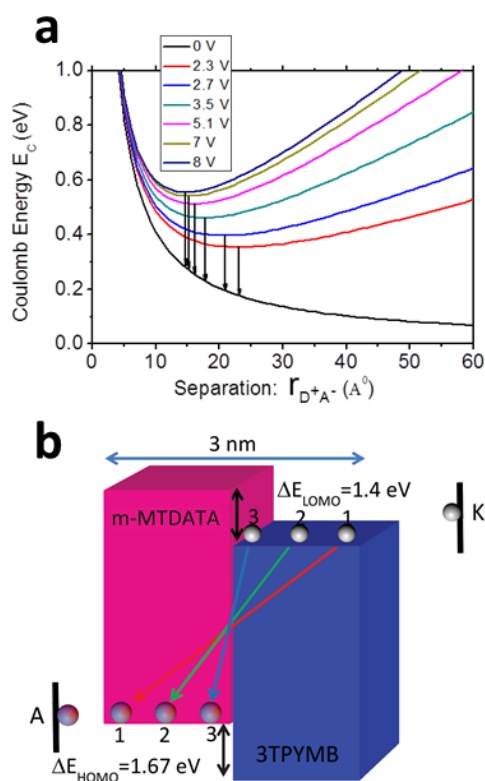


Figure 4. (a) Schematic Coulomb energy diagram as a function of ion-pair separation showing the relaxed exciplex transitions under different applied voltage (b) The energy level diagram of the donor m-MTDATA and the acceptor 3TPYMB, showing the large HOMO-LUMO energy off-set at the interface. The hypothetical locations 1, 2 and 3 for the electrons and holes within 3 nm interface section represent three selected positions that correspond to three applied voltages. Electron and hole at each specific separation may form an exciplex that emit light at specific wavelength depending on the electron-hole separation.

Voltage (V)	λ (nm)	E_c (eV)	$r_{D^+A^-}$ (nm)	$F \times 10^6$ (V/cm)	Effect. Thick. d (nm)
2.3	547	0.3669	2.234	0.8208	28

2.7	540	0.3963	2.07	0.9576	28.2
3.5	528	0.4485	1.828	1.2264	28.6
5.1	516	0.503	1.63	1.5433	33
7	509	0.536	1.53	1.7527	39.2
8	506	0.55	1.443	1.8943	42

*Table 1. The measured applied voltage and exciplex peak emission wavelength in double layer device, and the calculated parameters from the equations (5-7). The effective thickness for the field was calculated from V/F , where an average field thickness of ~ 33 nm.

From equations, 4 and 7, we see that the electron-hole separation is a linear function of the wavelength shift, so we can estimate the sensitivity of this method to be ~ 160 nm of spectrum shift per 1 nm of electron-hole separation change, effectively we can measure electron-hole separation to an accuracy of better than 10 pm. *However, a plot of equation 6 and 7 (Fig SI 5) shows a deviation from linearity at low applied voltage and this may be attributed to the effect of the build-in potential whose effect is significant only at low applied voltage. The accuracy of this method depends on the accuracy of identifying the peak emission wavelength, donor-acceptor HOMO-LUMO energy levels and also the accuracy in estimation of the organic relative dielectric constant.

In summary, we have designed a simple but novel method to study the characteristics of the exciplex state pinned at a donor-acceptor abrupt interface and the effect of an external electric field on these excited states. Because the exciplex states are pinned across the interface, there is a net directionality in the average dipole moments across the interface and so we can apply the field that adds to the electron-hole coulomb attraction and so reduce the electron-hole separation in each exciplex, an effective inverse of the 'Onsager processes normally studied in photodissociation experiments. We observed strong blue spectral shifts in the

electroluminescences of these heterojunction devices as a function of applied voltage, and we could obtain both the electron-hole separations and Coulomb potential. As the electron-hole separation decreases, from 2.3 nm to 1.5 nm as the applied field increased from 8×10^5 V/cm to 2×10^6 V/cm, the exciplexes gain local excited state character which increases the radiative decay rate and thus efficiency of emission. The magnitude of the blue shift is not dependent only on the electrical structure of the interface, but also on the relative geometrical structure of the donor and acceptor molecules at the interface as well as the characteristics of the applied field. This technique can be considered as an extremely sensitive method to study the physics of the exciplex excited state and allows us to control electro-hole separation to better than 10 pm.

Methods

m-MTDATA and 3TPYMB were purchased from Sigma-Aldrich and used without any further purification. Organic films of the individual compounds and of blended film 1:1 weight ratio for optical measurements were fabricated by spin coating method from a solution of CH_2Cl_2 at 10 mg/ml. Absorption and photoluminescence spectra of these films were recorded using UV-3600 Shimadzu spectrophotometer and Jobin Horiba Fluoromax 3 respectively. Time resolved spectra were obtained by exciting the sample with a 150 ps-pulsed, 10 Hz, 355 nm Nd:YAG laser. The emission was directed onto a spectrograph and gated iCCD camera (Stanford Computer Optics). The PL decay transients were obtained using exponentially increasing decay and integration times as previously described ^[30].

Single and double layers OLED devices were fabricated using pre-cleaned indium –tin-oxide (ITO) coated glass substrate patterned to form four pixels of 4x5 mm in 24x24 mm sample, purchased from Kinetic. The ITO thickness around 120 nm with a sheet resistance of $15 \Omega/\square$. The cleaned samples were exposed to UV-ozone for 10 min and porched by dry nitrogen. A hole-injection layer (HIL) of PEDOT:PSS (4083) of thickness 40 nm was spin coated at 5000

rpm for 1 min and then baked on a hotplate at 180 °C for 6 min to remove any remaining moisture. The small molecules and the cathode layers were thermally evaporated using the Kurt J. Lesker Spectros II deposition chamber at 10^{-6} mbar. All organic materials and aluminium were deposited at a rate of 1 Å/s. The Double layer devices were fabricated by thermally evaporated of 30 nm of m-MTDATA followed by 30 nm of 3TPYMB. For the single layer device the two compounds were co-evaporated in 1:1 ratio to form a film of 30 nm followed by 30 nm of 3TPYMB. The LiF layer of ~ 0.7 nm was evaporated at 0.1 Å/s and finally capped by 100 nm Al. The devices were then encapsulated with DELO UV curable epoxy (Katiobond) and a 12 x12 mm glass cover slide.

The current–voltage ($I-V$) characteristics and the emission intensities were measured in a calibrated Labsphere LMS-100 integrating sphere and the data acquisition was controlled using a home-written NI LabView program that controlled an Agilent Technologies 6632B power supply. The electroluminescence (EL) spectra were measured using an Ocean Optics USB 4000 CCD spectrometer supplied with a 400- μ m UV–vis fibre optic cable.

Acknowledgements

We thank the EPSRC for funding this work.

References

- [1] H. E. Katz, H. Jia, Annual Review of Materials Research 2009, 39, 71.
- [2] K. Vandewal, K. Tvingstedt, A. Gadisa, O. Inganas, J. V. Manca, Nat Mater 2009, 8, 904; H. Uoyama, K. Goushi, K. Shizu, H. Nomura, C. Adachi, Nature 2012, 492, 234; W. E. B. Shepherd, A. D. Platt, M. J. Kendrick, M. A. Loth, J. E. Anthony, O. Ostroverkhova, The Journal of Physical Chemistry Letters 2011, 2, 362.
- [3] S. A. Jenekhe, J. A. Osaheni, Science 1994, 265, 765.
- [4] K. Goushi, K. Yoshida, K. Sato, C. Adachi, Nat Photon 2012, 6, 253.
- [5] J. Li, H. Nomura, H. Miyazaki, C. Adachi, Chemical Communications 2014, 50, 6174.
- [6] V. Jankus, C.-J. Chiang, F. Dias, A. P. Monkman, Advanced Materials 2013, 25, 1455.
- [7] V. Jankus, P. Data, D. Graves, C. McGuinness, J. Santos, M. R. Bryce, F. B. Dias, A. P. Monkman, Advanced Functional Materials 2014, 24, 6178.
- [8] B. Zhao, T. Zhang, B. Chu, W. Li, Z. Su, H. Wu, X. Yan, F. Jin, Y. Gao, C. Liu, Scientific Reports 2015, 5, 10697; D. Yu, S. Fengbo, Y. Dan, Y. Yongqiang, C. Ping, D. Yahui, Applied Physics Express 2014,

- 7, 052102; H. Shin, S. Lee, K.-H. Kim, C.-K. Moon, S.-J. Yoo, J.-H. Lee, J.-J. Kim, *Advanced Materials* 2014, 26, 4730; Y.-S. Park, S. Lee, K.-H. Kim, S.-Y. Kim, J.-H. Lee, J.-J. Kim, *Advanced Functional Materials* 2013, 23, 4914.
- [9] J. J. Benson-Smith, J. Wilson, C. Dyer-Smith, K. Mouri, S. Yamaguchi, H. Murata, J. Nelson, *The Journal of Physical Chemistry B* 2009, 113, 7794.
- [10] C. Deibel, T. Strobel, V. Dyakonov, *Advanced Materials* 2010, 22, 4097.
- [11] I. R. Gould, R. H. Young, L. J. Mueller, A. C. Albrecht, S. Farid, *Journal of the American Chemical Society* 1994, 116, 8188.
- [12] E. M. Conwell, J. Perlstein, S. Shaik, *Physical Review B* 1996, 54, R2308.
- [13] H.-C. Lin, B.-Y. Jin, *Materials* 2010, 3, 4214.
- [14] S. Sharifzadeh, P. Darancet, L. Kronik, J. B. Neaton, *The Journal of Physical Chemistry Letters* 2013, 4, 2197.
- [15] M. Muntwiler, Q. Yang, W. A. Tisdale, X. Y. Zhu, *Physical Review Letters* 2008, 101, 196403.
- [16] A. A. Bakulin, A. Rao, V. G. Pavelyev, P. H. M. van Loosdrecht, M. S. Pshenichnikov, D. Niedzialek, J. Cornil, D. Beljonne, R. H. Friend, *Science* 2012, 335, 1340; A. E. Jailaubekov, A. P. Willard, J. R. Tritsch, W.-L. Chan, N. Sai, R. Gearba, L. G. Kaake, K. J. Williams, K. Leung, P. J. Rossky, X. Y. Zhu, *Nat Mater* 2013, 12, 66; B. Bernardo, D. Cheyns, B. Verreet, R. D. Schaller, B. P. Rand, N. C. Giebink, *Nat Commun* 2014, 5.
- [17] L. Onsager, *Physical Review* 1938, 54, 554.
- [18] H. Bassler, *Primary Photoexcitations in Conjugated Polymers: Molecular Exciton versus Semiconductor Band Model*, World Scientific, Singapore 1997; D. M. Pai, R. C. Enck, *Physical Review B* 1975, 11, 5163.
- [19] M. Yokoyama, Y. Endo, H. Mikawa, *Chemical Physics Letters* 1975, 34, 597.
- [20] A. C. Morteani, P. Sreearunothai, L. M. Herz, R. H. Friend, C. Silva, *Physical Review Letters* 2004, 92, 247402.
- [21] V. I. Arkhipov, E. V. Emelianova, H. Bässler, *Physical Review Letters* 1999, 82, 1321.
- [22] B. Briks J, *Photophysics of Aromatic Molecules*, Wiley-Interscience, London 1970.
- [23] R. J. Holmes, S. R. Forrest, Y.-J. Tung, R. C. Kwong, J. J. Brown, S. Garon, M. E. Thompson, *Applied Physics Letters* 2003, 82, 2422.
- [24] S.-J. He, D.-K. Wang, N. Jiang, J. S. Tse, Z.-H. Lu, *Advanced Materials* 2016, 28, 649.
- [25] D. Beljonne, J. Cornil, L. Muccioli, C. Zannoni, J.-L. Brédas, F. Castet, *Chemistry of Materials* 2011, 23, 591.
- [26] G. G. Malliaras, J. R. Salem, P. J. Brock, J. C. Scott, *Journal of Applied Physics* 1998, 84, 1583.
- [27] J. Rommens, A. Vaes, M. Van der Auweraer, F. C. De Schryver, H. Bässler, H. Vestweber, J. Pommerehne, *Journal of Applied Physics* 1998, 84, 4487; A. Weller, in *The Exciplex*, (Ed: M. G. R. Ware), Academic Press, 1975, 23.
- [28] T. Granlund, L. A. A. Pettersson, M. R. Anderson, O. Inganäs, *Journal of Applied Physics* 1997, 81, 8097; J. Kalinowski, G. Giro, M. Cocchi, V. Fattori, P. Di Marco, *Applied Physics Letters* 2000, 76, 2352.
- [29] M. Yokoyama, Y. Endo, H. Mikawa, *Bulletin of the Chemical Society of Japan* 1976, 49, 1538.
- [30] C. Rothe, A. P. Monkman, *Physical Review B* 2003, 68, 075208.

Supporting Information

Electric Field Induce Blue Shift and Intensity Enhancement in 2D Exciplex Organic Light Emitting Diodes ; Controlling Electron-Hole Separation.

Hameed A. Al Attar and Andy P. Monkman

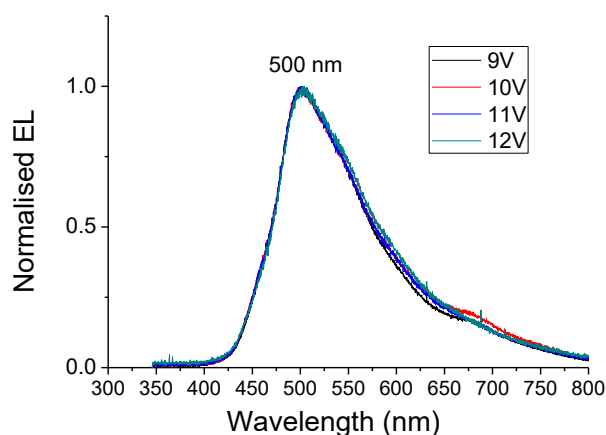


Fig. SI-1. Normalised EL emission for applied voltage above 8 V in DL device shows the spectra over-laps and the convergence of the blue emission shift at 500 nm.

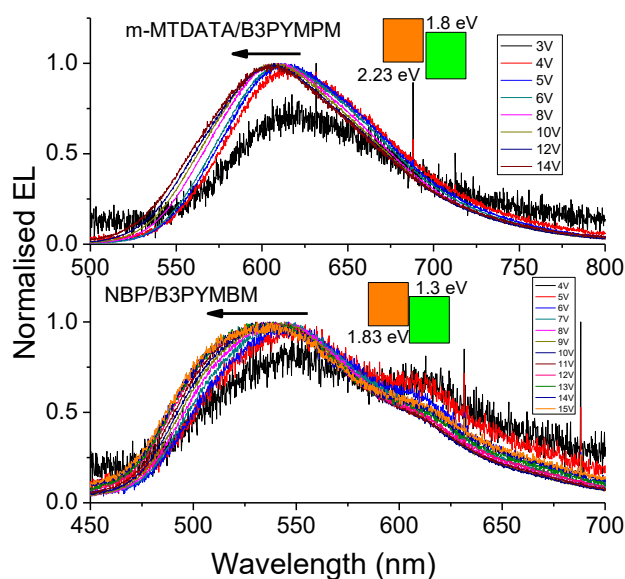


Fig. SI-3 EL emission from OLED devices of similar structure to that used in the manuscript using two D/A pairs, m-MTDATA/ B3PYMPM and NBP/B3PYMBM, showing the blue

emission shift with the applied voltage. The acceptor B3PYMBM where used her to form larger HOMO-LUMO energy offset than that formed between m-MTDATA/3TPYMB but the blue shift is much smaller, which indicate that the blue emission shift is strongly dependence on the geometric structure of the donor and acceptor molecules at the interface.

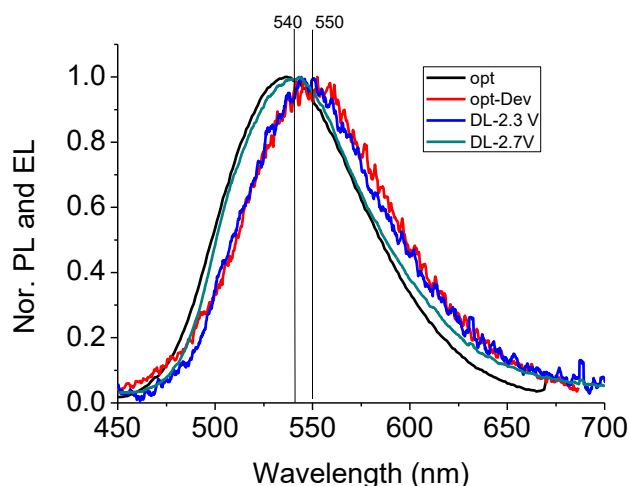


Fig. SI-3. The PL and EL emission profiles for optically excited and electrically excited blend film of m-MTDATA: 3TPYMB on quartz substrate and as a device structure with electrodes, to explore the build-in potential effect on the emission peaks.

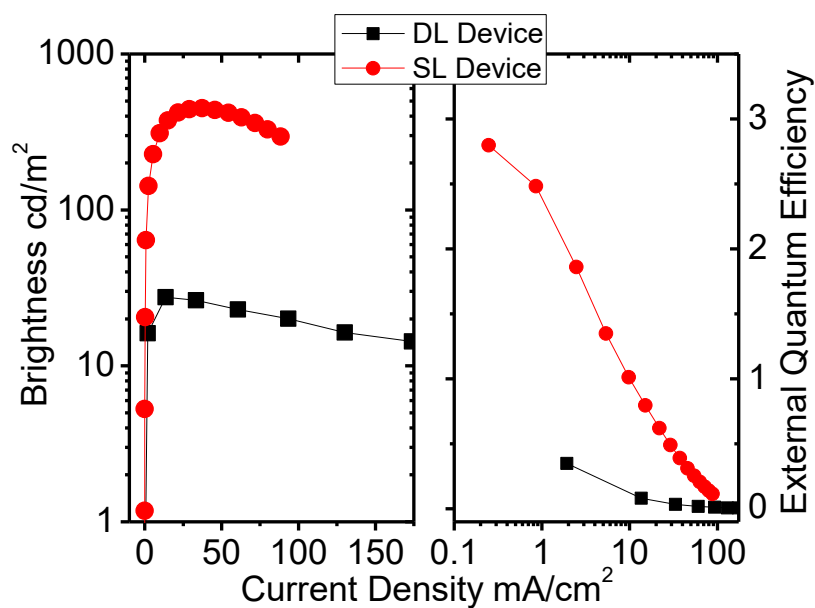


Fig. SI-4 Brightness and External quantum efficiency vs current density for single and double layers devices

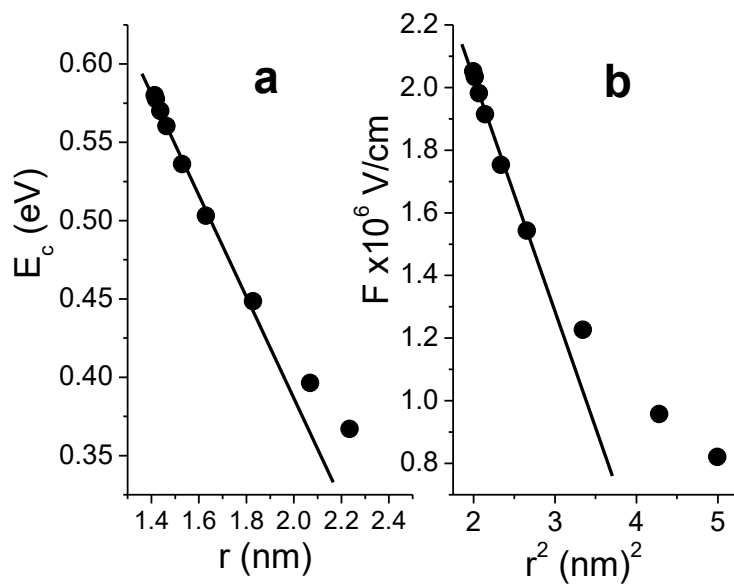


Fig SI-5 A plots of equation 7 (a) and equation 6 (b) showing a deviation from linearity at low applied voltage and this may be attributed to the effect of the build-in potential